Hybrid thermochemical cycles for power and cold cogeneration: thermodynamic analysis and dynamic performances

Alexis Godefroy, Maxime Perier-Muzet, Pierre Neveu, Nathalie Mazet

Hybrid thermochemical cycles for power and cold cogeneration: thermodynamic analysis and dynamic performances

Godefroy, Alexis[1,2], Perier-Muzet, Maxime[1,2], Neveu, Pierre[2], Mazet, Nathalie[1]

[1] *CNRS-PROMES Laboratoire PROcédés, Matériaux et Energie Solaire, 66100 Perpignan, France*
(corresponding author: alexis.godefroy@promes.cnrs.fr)
[2] *Université de Perpignan Via Domitia, 66100 Perpignan, France*

Abstract:
Based on the coupling of a thermochemical sorption cycle with an expansion device, five operating modes are presented for low-grade heat storage and conversion into power and cold. Considering $CaCl_2$,(8/4)NH_3 as reactant, the performances of these hybrid cycles are presented. The simultaneous power and cold production mode is the most promising one. Its energy and exergy efficiencies reach 0.50 and 0.33, respectively, and its energy storage density 151.4 kWh/m^3_{system}. The study of the dynamic behavior of this cycle shows that a suitable control of the expander leads to stable power and cold outputs of 490 W and 8 kW for 3 hours, using 0.19 m^3 reactive composite.

1 Introduction

Industrial waste heat at low temperatures (lower than 250 °C) is a huge heat source. Several cycles have been developed to recover this heat, such as ORC for electricity production or sorption cycles for cold production and storage purposes. The hybrid thermochemical cycles based on solid/gas reactions combine power and cold production with a storage feature, by inserting an expansion device in a thermochemical cycle. So far, very limited research has been carried out on this kind of hybrid cycles, despite their attractive storage ability. In the early work of Ziegler et al. [1], a re-evaluation of the Honigmann process was proposed, leading to a broad approach of hybrid sorption cycles involving an expansion device for power production. Later, Bao et al. [2] investigated their dynamic behavior. Their experimental study [3] showed that power output is very unstable without any external control of the expander behavior, due to the strong coupling between expansion and reaction kinetics. Therefore, managing the dynamic behavior of such hybrid thermochemical cycle is still a key issue. In this paper, 5 ways of hybridizing a thermochemical cycle with an expander are presented. The significant results of the thermodynamic and dynamic studies are depicted, focusing on $CaCl_2$ (8/4)NH_3 as solid reactant of the sorption process.

2 Operating modes of hybrid thermochemical cycles

Classical thermochemical sorption cycles are characterized by their discontinuous operation, which provides their storage feature: a cycle involves a charging step (endothermal decomposition reaction) and a discharging step (exothermal synthesis reaction). Hybridizing a thermochemical sorption cycle consists in inserting an expansion device on the gas flow between its classical components. Five different operating modes have been identified, they are depicted in Figs. 1 (general working principle) and 2 (thermodynamic paths). They are sorted according to their shares of power and cold in the overall production:

- **Prevailing cold production modes**: the expander is inserted either in the charging step, in the discharging step, or in both steps. These 3 modes are thoroughly investigated in [4]. They are named respectively:

- separated power and cold mode: $W_{ch} \neq 0$ and $W_{disch} = 0$ (in Figure 2: Charge (b) and Discharge (c)),
- simultaneous power and cold mode: $W_{disch} \neq 0$ and $W_{ch} = 0$ (in Figure 2: Charge (a) and Discharge (d)),
- combined power and cold production mode: $W_{ch} \neq 0$ and $W_{disch} \neq 0$) (in Figure 2: Charge (b) and Discharge (d)).

- **Prevailing power generation modes**: in the discharging step, the constraint of cold production is removed, which allows increasing evaporator pressure (point 4') and inserting an expander between evaporator and reactor (points 5'-6'). Heat from the reactor (point 7') is provided to the evaporator to achieve an original autothermal power production step. We note that such autothermal process is close to the above-mentioned Honigmann process for electricity production. A residual cold production occurs at the expander outlet (point 6'). An expander can also be inserted in the charging step, as described above. This leads to two operating modes:

- discharge power generation mode: $W_{disch} \neq 0$ and $W_{ch} = 0$ (in Figure 2: Charge (a) and Discharge (e)),

- **combined** charge and discharge power generation mode: $W_{ch} \neq 0$ and $W_{disch} \neq 0$ (Charge (b) and Discharge (e)).

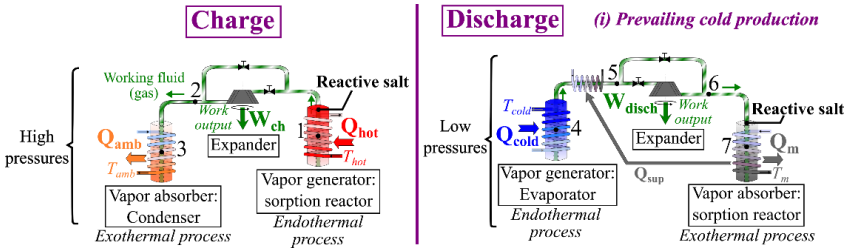

Figure 1 – Operating modes of hybrid thermochemical cycles: working principle. Valves enable the actuation or bypass of the expander.

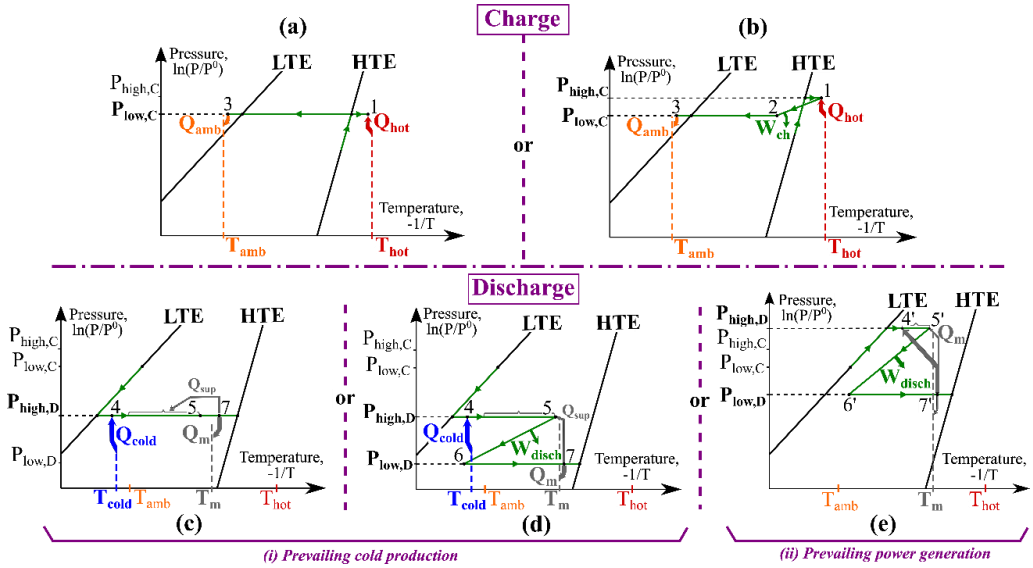

Figure 2 – Operating modes of hybrid thermochemical cycles: thermodynamic paths in Clausius-Clapeyron diagrams. LTE: Low Temperature Equilibrium, liquid/vapor phase change equilibrium of the working fluid. HTE: High Temperature Equilibrium, chemical reaction equilibrium of the reactant.

3 Framework and main results of the study

3.1 Thermodynamic study

The thermodynamic study is based on usual assumptions (steady-state process, heat losses and pressure drops inside components are neglected). It is detailed in a previous work [4]. Several temperature pinches are set for heat exchanges and for the deviation from chemical reaction equilibrium line (HTE line). The cold source and ambient sink temperatures are set at T_{cold} = 0 °C and T_{amb} = 20 °C, while the required heat source temperature T_{hot} depends on reactive salt and operating mode. Thermodynamic analyses were conducted for the 5 modes. Four key performance indicators were selected (Table 1). The power production ratio τ_w gives the share of power in the total output. The energy efficiency η_I of these cogeneration cycles involves all energy outputs over one complete cycle ($W = W_{ch}+W_{disch}$ and Q_{cold}). The exergy efficiency η_{ex} allows a fair comparison between the operating modes despite the various shares of cold and mechanical work outputs. The storage performance indicator ESD (Energy Storage Density) involves the production in discharging step and the volume of storage components (reactor – metal wall, anhydrous reactive salt and porous volume, considering a global porosity of 0.7 – and NH_3 tank).

Power production ratio	Energy efficiency	Exergy efficiency	Energy Storage Density
$\tau_w = \frac{\lvert W\rvert}{\lvert W\rvert + Q_{cold}}$	$\eta_I = \frac{\lvert W\rvert + Q_{cold}}{Q_{hot}}$	$\eta_{ex} = \frac{\lvert W\rvert + \lvert Ex_{cold}\rvert}{Ex_{hot}}$	$ESD = \frac{\lvert W_{disch}\rvert + Q_{cold}}{V_{stor}}$

Table 1 – Definition of four key performance indicators to characterize the operation of the hybrid thermochemical cycles.

3.2 Dynamic modelling

To predict the dynamics of hybrid thermochemical cycles, models were developed for each component (reactor, condenser, evaporator, expander), accounting for their respective dynamic behaviors. In each component, internal

variables (thermodynamic state of the gas, wall temperature, reaction advancement …) were considered uniform (0D modelling). The model of the reactor includes energy and mass balances, solid/gas reaction kinetics, and an ideal gas assumption. The works of Castaing et al. [5] and Bao et al. [2] provide more details on such 0D approach for thermochemical systems. Realistic heat transfer coefficients have been used (100 $W.m^{-2}.K^{-1}$ for reactive bed/wall, 1000 $W.m^{-2}.K^{-1}$ for wall/heat exchanger). As a first approach, the expander is supposed to operate in steady-state and its global performance is described by two efficiencies: isentropic efficiency η_{is} and volumetric efficiency η_v. Moreover, its exhaust pressure is fixed to simulate user control. Finally, $CaCl_2$ (8/4)NH_3 emerged as a good candidate and a well-known reactant [4]. Thus, the following results are based on this reactive salt.

3.3 Thermodynamic study: results for all operating modes

The main results are gathered in Table 2: heat source temperature T_{hot} and key performance indicators (see §3.1).

	Prevailing cold production			Prevailing power generation	
	Separated mode	Simultaneous	Combined	Discharge mode	Combined
T_{hot} (°C)	138	108	138	108	138
τ_w (%)	10.9	5.0	14.8	53.2	70.7
η_I (-)	0.44	0.42	0.45	0.08	0.12
η_{ex} (-)	0.26	0.22	0.33	0.20	0.31
ESD^* (kWh/m^3_{system})	74.4	151.4	107.9	33.0	28.1

*Table 2 – Results of the thermodynamic analyses for the 5 operating modes. Selected reactant: $CaCl_2$ (8/4)NH_3. * ESD is computed for $CaCl_2$ (8/2)NH_3*

The 3 operating modes involving a non-isobaric charging step (separated mode, combined power and cold mode, combined charge and discharge mode) require a higher heat source temperature (T_{hot}=*138°C*) than the other operating modes (T_{hot}=*108°C*). As expected, power production ratios are higher for prevailing power modes ($\tau_w \approx$ *53-71 %*, against *5-15 %* for prevailing cold modes). Moreover, energy efficiencies are much higher for prevailing cold modes ($\eta_I \approx$ *0.42-0.45*, against *0.08-0.12* for prevailing power modes). The difference no longer exists for exergy efficiencies, because this indicator takes account of the high share of power provided by the prevailing power modes. Finally, the highest Energy Storage Density is reached by the simultaneous mode because all useful effects (cold and power) are produced during the discharging step. In view of this good storage performance, simultaneous mode has been selected as case study for the dynamic modelling hereafter.

3.4 Dynamic modelling: results for simultaneous mode

The simultaneous mode appears as the most promising mode. Thus, its dynamic behavior during the discharging step is investigated. The components (evaporator, superheater, expander and reactor with 0.19 m^3 of composite: see Fig. 1) initially rest at ambient temperature. The simulation begins when the evaporator is connected to the cooling loop (at T_{cold} = *0 °C*) and mass connections between the components (valves) are open. In Fig. 3a, output powers during discharging step (right side) and input thermal power during charging step (right side) are plotted over time. Fig. 3b displays the operating pressures (left side), temperatures and reaction advancement (right side). Regarding output thermal and mechanical powers, a peak is observed at the beginning of the discharging step (Figure 3a: more than 27 kW cold production and 1 kW power production). It lasts less than 2 minutes. Then, the non-equilibrium stage that is reached is close to a steady-state stage: during this stage, cold power mean value is 8 kW and mechanical power mean value is 490 W. Finally, a decrease occurs at about 175 min, caused by the decrease in solid/gas reaction kinetics: the reaction is almost complete (advancement reaches 0.9, see Figure 3b). At the beginning of the simulation, the evaporator temperature T_{ev} suddenly drops (Figure 3b) because of two main factors: (i) the mass connection with the other components (especially the reactor resting at a much lower pressure) which brings the evaporator out of its liquid/vapor equilibrium and creates a suction effect, and (ii) the thermal connection with the cooling loop. This causes the sharp increase in thermal and mechanical powers.

Regarding pressures, a pressure control has been implemented so that the expander low pressure is fixed at 1.9 bar. During the operating stage that is close to a steady-state stage, the evaporator lies at high pressure $P_{high,D} = P_{ev}$ = 4 bar and the reactor lies at low pressure $P_{low,D} = P_r$ = 1.9 bar (the expander pressure ratio is 2).

Finally, using the data from this dynamic study, the energy and exergy performance indicators listed in Table 1 have been computed: they reach $\eta_I=0.50$, $\eta_{ex}=0.33$ and $\tau_w=5.6$ %. Although relatively close to the estimates derived from thermodynamic study (Table 2, simultaneous mode), these performance values are slightly higher because the temperature pinches are lower than the ones set for the thermodynamic study.

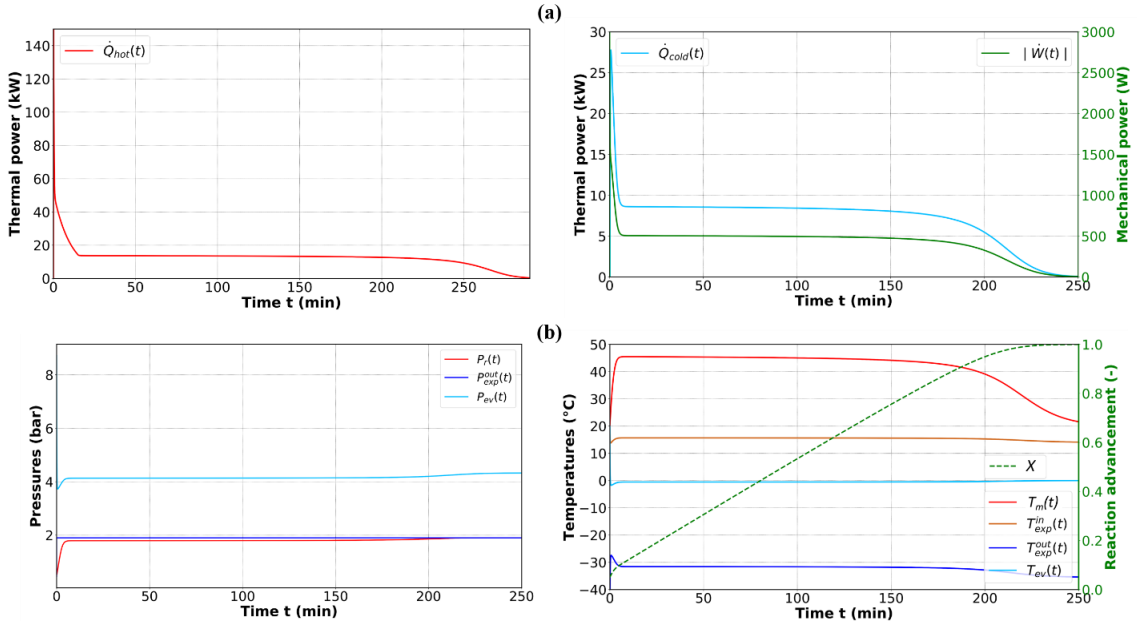

Figure 3 – Simultaneous mode (using $CaCl_2$ (8/4)NH_3 as reactant): main results of the dynamic study. (a) thermal and mechanical powers during charging (left side) and discharging (right side) steps (b) Operating pressures (left side), temperatures and reaction advancement (right side) during discharging step.

4 Conclusions

In this paper, five operating modes of hybrid thermochemical cycles were introduced, targeting low-grade heat storage and cogeneration of power and cold. $CaCl_2$ (8/4)NH_3 was chosen as reactive salt. A thermodynamic analysis allowed the determination of their energy, exergy and storage performances. The simultaneous power and cold production mode appeared as very promising, especially in terms of energy storage density. The dynamic behavior of this mode was investigated by means of a dynamic model. The first results of this dynamic study highlighted the highly dynamic behavior of the process at the beginning of the discharging step. The global energy and exergy performances obtained with the dynamic study are promising, in line with the results of the thermodynamic analysis: energy and exergy efficiencies reach 0.50 and 0.33, respectively.

These first results suggest a strong coupling between reactor and expander, which needs further investigations: the increase in pressure ratio across the expander (linked to the increase in mechanical power) is competing with the increase in pressure deviation from the thermodynamic equilibrium of the reactor (linked to the increase in solid/gas chemical reaction kinetics). Using mean mechanical power as objective function, the existence of an optimal exhaust pressure of the expander is under study. An experimental proof-of-concept is currently under development, it will integrate a control of the expander to achieve optimal and stable power output.

5 Acknowledgment

Alexis Godefroy receives a PhD grant from the French Ministry of National Education (No. 2017-09-ED.305).

6 List of References

[1] Ziegler, F., Jahnke, A., Karow, M. (2009): Re-evaluation of the Honigmann-process: thermo-chemical heat store for the supply of electricity and refrigeration. *Vortrag und Proc. of Heat Powered Cycles Conf.*, Berlin.

[2] Bao, H., Wang, Y., Roskilly, AP. (2014): Modelling of a chemisorption refrigeration and power cogeneration system. *Applied Energy*, vol. 119, pp. 351-62.

[3] Bao, H., Wang, Y., Charamboulos, C., Lu, Z., Wang, L., Wang, R., et al. (2014): Chemisorption cooling and electric power cogeneration system driven by low grade heat. *Energy*, vol. 72, pp. 590-8.

[4] Godefroy, A., Perier-Muzet, M., Mazet, N. (2019): Thermodynamic analyses on hybrid sorption cycles for low-grade heat storage and cogeneration of power and refrigeration. *Applied Energy*, vol. 255.

[5] Castaing-Lasvignottes, J., Neveu, P. (1997): Development of a numerical sizing tool for a thermochemical transformer (Parts I and II). *Applied Thermal Engineering*, vol. 17, pp. 501-36.²